Preparation, Structure, and Thermal Stability of New $Ni_xCo_{1-2x}Mn_x(OH)_2$ ($0 \le x \le 1/2$) Phases

S. Jouanneau and J. R. Dahn*

Department of Physics, Dalhousie University, Halifax, Nova Scotia, B3H 3J5, Canada

Received August 6, 2002. Revised Manuscript Received November 6, 2002

The preparation, characterization, and thermal stability of $Ni_xCo_{1-2x}Mn_x(OH)_2$ ($0 \le x \le 1/2$) is reported. These hydroxides are prepared by coprecipitation as the first step in the preparation of the corresponding $Li[Ni_xCo_{(1-2x)}Mn_x]O_2$ ($0 \le x \le 1/2$) oxides. Precipitates dried at room temperature adopt the hexagonal CdI_2 structure. Thermal studies show that the hexagonal CdI_2 type (RT) structure transforms to a cubic spinel-type solid solution $(Ni_xCo_{(1-2x)}Mn_x]_3O_4$ ($0 \le x \le 3/8$) above about 150 °C that becomes well-crystallized at 600 °C. An intermediate turbostratic structure phase occurs between room temperature and 150 °C. This phase is present in small amounts in room-temperature-dried $Ni_xCo_{1-2x}Mn_x(OH)_2$ materials with $x \ge 3/8$. The results show that the drying method of the precipitate induces different phases with different bulk and tap density. This could have a major influence on the morphology, composition, density, and cell performance of $Li[Ni_xCo_{(1-2x)}Mn_x]O_2$ ($0 \le x \le 1/2$) oxides obtained from these dried precipitates.

Introduction

Many recent reports address the problem of synthesizing a layered cathode material that is cheaper, of higher capacity, and safer than $LiCoO_2$, $LiNiO_2$, and $Li(Ni,Co)O_2$.[1−12] $Li[Co_{1/3}Ni_{1/3}Mn_{1/3}]O_2$,[13] $Li[Ni_xLi_{(1/3-2x/3)}Mn_{(2/3-x/3)}]O_2$ ($0 \le x \le 1/2$),[14] and $Li[Ni_xCo_{(1-2x)}Mn_x]O_2$ ($0 \le x \le 1/2$)[15] layered cathode materials have also been developed.

These last compounds adopt the α-$NaFeO_2$ type structure and can be regarded as the substitution of Ni^{2+} and Mn^{4+} (1:1) for Co^{3+} in $LiCoO_2$.[16] $Li[Ni_xCo_{1-2x}Mn_x]O_2$ with $x = 1/4$ can deliver a stable capacity of 160 mAh/g using a specific current of 40 mA/g when it is cycled between 2.5 and 4.4 V.[16] $Li[Ni_xCo_{1-2x}Mn_x]O_2$ with $x = 3/8$ can give a capacity of about 150 mAh/g at 30 °C and 165 mAh/g at 55 °C between 2.5 and 4.4 V using a specific current of 40 mA/g.[16] DSC results for electrodes of $Li[Ni_xCo_{1-2x}Mn_x]O_2$ wetted with electrolyte indicate that $Li[Ni_xCo_{1-2x}Mn_x]O_2$ with $x = 1/4$ and $3/8$ are significantly safer than $LiCoO_2$.[15] Ni and Mn are less expensive than Co, therefore $Li[Ni_xCo_{1-2x}Mn_x]O_2$ with $x = 1/4$ and $3/8$ are promising materials to replace $LiCoO_2$. One inconvenient feature of these compounds is the low tap density achieved in typical laboratory synthesis that is not suitable for electrode production in practical Li-ion cells.[17]

These compounds are prepared by a mixed hydroxide method[15] that consists of two steps. The first is a coprecipitation of transition metal salts in a stirred solution of LiOH. This causes the precipitation of $M(OH)_2$ (M = Mn, Ni, and Co) with an homogeneous cation distribution. The second step consists of mixing the precipitate dried at 160 °C overnight with the stoichiometric amount of $Li(OH)\cdot H_2O$ and heating the powder or pellet in air at a given temperature. Both steps could have a great influence on properties of $Li[Ni_xCo_{1-2x}Mn_x]O_2$, such as structure, composition, density, and electrochemical performance. To improve these cathode materials, we focused initially on the first step. That is, we studied the preparation and thermal stability of the precipitate $Ni_xCo_{1-2x}Mn_x(OH)_2$ ($0 \le x \le 1/2$).

Experimental Section

$LiOH\cdot H_2O$ (98%+, Aldrich), $CoSO_4\cdot 7H_2O$ (99%+, Sigma), $NiSO_4\cdot 6H_2O$ (98%, Alpha Aesar), and $MnSO_4\cdot H_2O$ (Fisher Scientific) were used as starting materials. The $Ni_xCo_{1-2x}Mn_x(OH)_2$ samples were prepared by coprecipitation as described by the first step of the "mixed hydroxide" method.[15] A 100-mL

* To whom correspondence should be addressed. E-mail: jeff.dahn@dal.ca.

(1) Armstrong, A. R.; Bruce, P. G. *Nature* **1996**, *381*, 499.
(2) Dahn, J. R.; Zheng, T.; Thomas, C. L. *J. Electrochem. Soc.* **1997**, *145*, 851.
(3) Dahn, J. R.; Zheng, T. U.S. patent 5,900,385, 1999.
(4) Gao, Y.; Yakovleva, M. V.; Ebner, W. B *Electrochem. Solid-State Lett.* **1998**, *1*, 117.
(5) Jang, Y.; Huang, B.; Chiang, Y. M.; Sadoway, D. R. *Electrochem. Solid-State Lett.* **1998**, *1*, 13.
(6) Paulsen, J. M.; Thomas, C. L.; Dahn, J. R. *J. Electrochem. Soc.* **2000**, *147*, 861.
(7) Desilvestro, H.; Ammundsen, B.; Hassell, D.; Pickering, P.; Steiner, R.; Davidson, I.; Grincourt, Y.; Kargina, I. *The 10th International Meeting on Lithium Batteries*; Como, Italy, May 28−June 2, 2000.
(8) Paulsen, J. M.; Ammundsen, B.; Desilvestro, H.; Steiner, R.; Hassell, D. *Abstract No. 71, The 198th Meeting of the Electrochemical Society*; Phoenix, AZ, Oct. 22−27, 2000.
(9) Cho, J.; Park, B. *Electrochem. Solid-State Lett.* **2000**, *3*, 355.
(10) Cho, J.; Kim, Y. J.; Park, B. *Chem. Mater.* **2000**, *12*, 3788.
(11) Numata, K.; Sakaki, C.; Yamanaka, S. *Chem. Lett.* **1997**, 725.
(12) Numata, K.; Sakaki, C.; Yamanaka, S. *Solid State Ionics* **1999**, *117*, 257.
(13) Ohsuku, T.; Makimura, Y. *Chem. Lett.* **2001**, *7−5*, 642.
(14) Lu, Z.; MacNeil, D. D.; Dahn, J. R. *Electrochem. Solid-State Lett.* **2001**, *4* (11), A191.
(15) Lu, Z.; MacNeil, D. D.; Dahn, J. R. *Electrochem. Solid-State Lett.* **2001**, *4* (12), A200.
(16) MacNeil, D. D.; Lu, Z.; Dahn, J. R. *J. Electrochem. Soc.* **2002**, *149* (10), A1332.
(17) Von Sacken, U. *E-One/Moli Energy*, July 2001, private communication.

10.1021/cm020818e CCC: $25.00 © 2003 American Chemical Society
Published on Web 01/01/2003

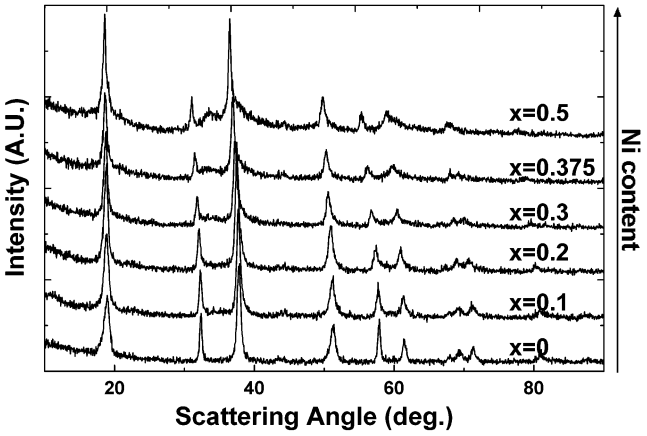

Figure 1. Powder X-ray diffraction profiles of $Ni_xCo_{1-2x}Mn_x(OH)_2$ dried at room temperature overnight with $0 \le x \le 1/2$ indicated.

aqueous solution of the transition metal sulfates (MSO_4 total concentration equal to 1 M) was dripped into 250 mL of a stirred solution of 1 M LiOH, using an electronic metering pump (LMI, Milton−Roy), with a constant speed and stroke leading to 1 h of coprecipitation. This should cause the precipitation of $M(OH)_2$ (M = Mn, Ni, and Co) with a homogeneous cation distribution. The beaker containing the starting transition metal sulfate solution and the pump tubes were washed with distilled water for 15 min to ensure that all the transition metal sulfates were added to the LiOH solution. The precipitate was filtered out and washed five times with additional distilled water to remove the residual Li salts (LiOH, SO_4^{2-} ions, or formed Li_2SO_4). The precipitate was dried in air at room temperature overnight. The dried precipitate was a "cake" resulting from the filtration process. A gentle grinding of 5 min with an automatic grinder (agate mortar with pestle) was used to disperse the powder (disagglomerate).

X-ray diffraction was made using a JD2000 diffractometer equipped with a Cu target X-ray tube and a diffracted beam monochromator. When the materials were single phase and adopted the hexagonal CdI_2 structure (space group *C*-3*m*, 164) or the cubic spinel structure (space group *Fd*3*m*, 227), lattice constants were determined by least squares refinement to the positions of at least 6 Bragg peaks. TEM experiments to examine sample morphology were performed with a FEI Tecnai-12 microscope (80 kV).

TGA measurements were performed in air with TA Instruments TGA 51 thermogravimetric analyzer at 5 K·min^{-1}.

The tap density of the sieved powder samples (less than 75 micrometers) was measured by placing a known mass of the powder in a vial and tapping it 50 times on a lab bench. The resulting volume of the powder in the tubes was determined and the tap density was calculated. Some measurements have been reproduced twice and we consider the error to be ±0.1 g/cm^3.

Results and Discussion

Figure 1 shows typical X-ray diffraction patterns of the $Ni_xCo_{1-2x}Mn_x(OH)_2$ coprecipitates obtained for $0 \le x \le 1/2$ and dried at room temperature overnight. Well-crystallized X-ray diagrams (Figure 1) were obtained for $0 \le x \le 1/2$. There is a smooth shift of the Bragg peaks as a function of the Ni (Mn) content, *x*. In all cases, the peaks can be indexed based on the hexagonal CdI_2 structure. Therefore, we could obtain the mixed hydroxides. This is also well illustrated by the TEM picture (Figure 2) showing well-defined hexagonal crystals for the composition $x = 3/8$. Nevertheless, we can distinguish some broad Bragg peaks between 30° and 40° and at around 60° (2θ values) for $x \ge 3/8$. This can be explained

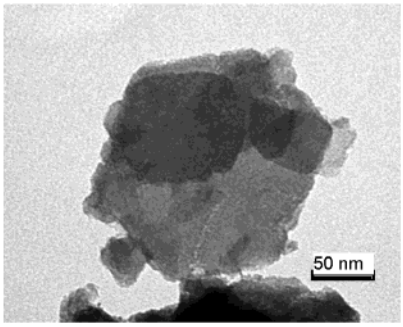

Figure 2. TEM picture of $Ni_xCo_{1-2x}Mn_x(OH)_2$ with $x = 3/8$.

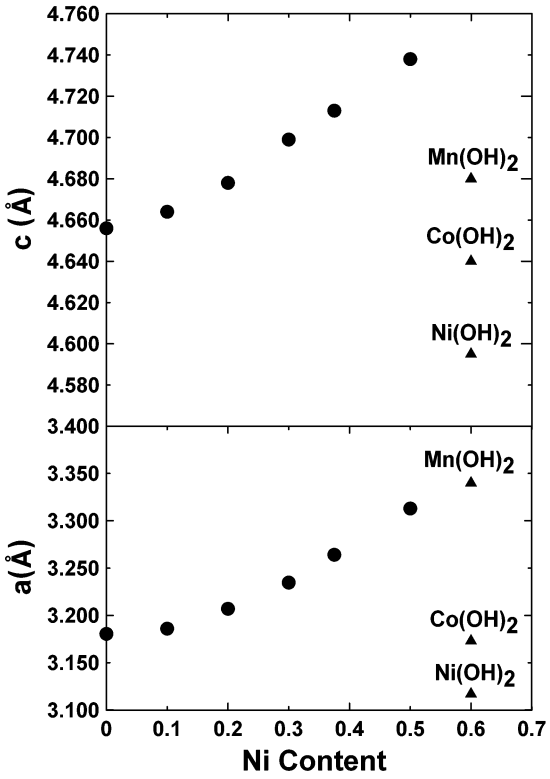

Figure 3. Lattice constants variation (circles) obtained from the powder X-ray patterns of $Ni_xCo_{1-2x}Mn_x(OH)_2$ ($0 \le x \le 1/2$), refined in the hexagonal cell of $Co(OH)_2$. Lattice constants of $M(OH)_2$ with M = Mn, Co, or Ni[19] are indicated as triangles for comparison.

by a turbostratic phase, such as the one proposed by Le Bihan[18] for the $Ni(OH)_2$ structure, that seems to appear when the Ni content increases. For the high Ni (Mn) content composition, the pristine CdI_2 structure is not so stable. The appearance of the turbostratic phase does not imply inhomogeneous cation distribution, only defects in the layered structure. Storage of a low Ni (Mn) content sample for a few weeks at room temperature also induces the appearance of small broad extra peaks from the turbostratic phase.

Lattice constants of all the $Ni_xCo_{1-2x}Mn_x(OH)_2$ mixed hydroxides ($0 \le x \le 1/2$) have been determined using the CdI_2 structure type. Figure 3 shows the lattice constants versus *x*. As the Mn and Ni contents increase there is a linear increase in both *a* and *c*. This is expected based on the larger ionic radii of Mn^{2+} (r = 0.80 Å) compared to that of Co^{2+} (r = 0.74 Å). The lattice

(18) Le Bihan, S.; Foglarz, M. *Electrochim. Acta* **1973**, *18*, 123.

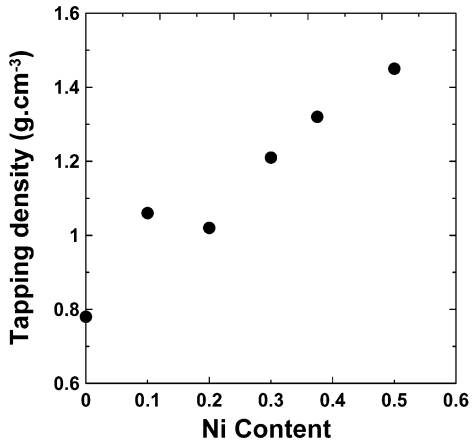

Figure 4. Tap density of $Ni_xCo_{1-2x}Mn_x(OH)_2$ ($0 \le x \le {}^1/_2$).

constant *a* increases from the value for $Co(OH)_2$ (a = 3.173 Å [19]) and tends to the larger value found for $Mn(OH)_2$ (a = 3.340 Å [19]). The lattice constant *c* increases linearly as well, but in this case the parameter is always higher than reference values for the pure Ni and Co hydroxides (c = 4.595 and 4.640 Å, respectively[19]). It even becomes larger than the *c* axis of $Mn(OH)_2$ (c = 4.680 Å[19]) for $x > 0.3$. This might suggest the presence of intercalated water or anionic species.

Figure 4 shows the tap density of the $Ni_xCo_{1-2x}Mn_x(OH)_2$ mixed hydroxides ($0 \le x \le {}^1/_2$) plotted versus *x*. There is a linear increase of the tap density with *x* from 0.78 g·cm^{-3} (x = 0) to 1.45 g·cm^{-3} (x = 0.5). This kind of evolution could have a direct consequence on tap density of the $Li[Ni_xCo_{(1-2x)}Mn_x]O_2$ oxides obtained from these hydroxides dried at room temperature.

In an attempt to explain the extra broad Bragg peaks that appear for $x > 0.375$, and the large *c* axis for the same compositions, we studied the thermal stability of the mixed hydroxides. We selected the composition $x = {}^3/_8$ for which we could already distinguish some extra broad Bragg peaks and which has a *c* axis larger than that of $Mn(OH)_2$.

Figure 5 shows X-ray diffraction patterns for $Ni_xCo_{(1-2x)}Mn_x(OH)_2$ with x = 0.375 as a function of drying temperature. Figure 6 shows the TGA profile for $Ni_xCo_{(1-2x)}Mn_x(OH)_2$ with $x = {}^3/_8$ (a) compared to that of a homemade $Co(OH)_2$ compound (b), and to that of a commercial β-$Ni(OH)_2$ (c). For these three compounds we indicate different mass loss regions (noted by either 1, 2, or 3) in Figure 6 attributed to each compound (noted by a, b, or c).

At room temperature (Figure 5) we clearly have the CdI_2 structure type with some broad extra peaks, particularly between 30° and 40°. An X-ray pattern of $Co(OH)_2$ prepared the same way is shown at the bottom of Figure 5 for comparison. When the drying temperature increases to 50 °C, we can no longer distinguish the entire CdI_2 diagram but only the first (001) peak, shifted toward higher angle, and some broad peaks that seem to be the same as those that already were present in the RT diagram. The shift of the (001) peak could indicate that a small amount of intercalated water was removed from the initial compound. This interpretation is consistent with the TGA profile (Figure 6a) that

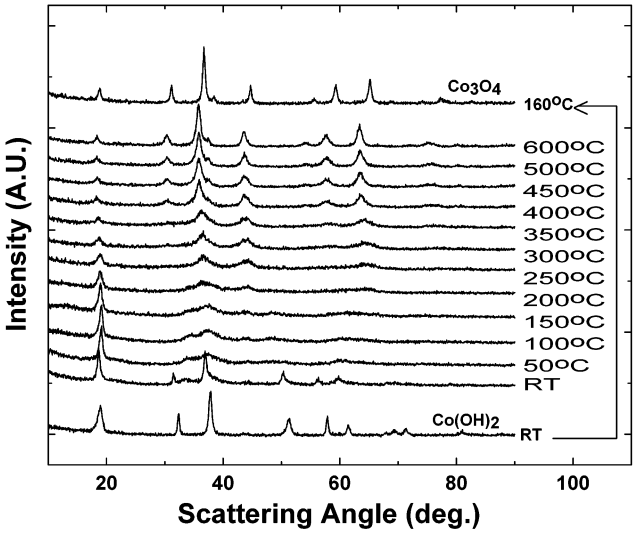

Figure 5. Variation of the powder X-ray diffraction profiles of $Ni_xCo_{(1-2x)}Mn_x(OH)_2$ with $x = {}^3/_8$ as a function of heating temperature from RT to 600 °C. The $Co(OH)_2$ (RT) and Co_3O_4 (previous one dried at 160 °C overnight) powder X-ray diffraction profiles are indicated at the bottom and top for comparison.

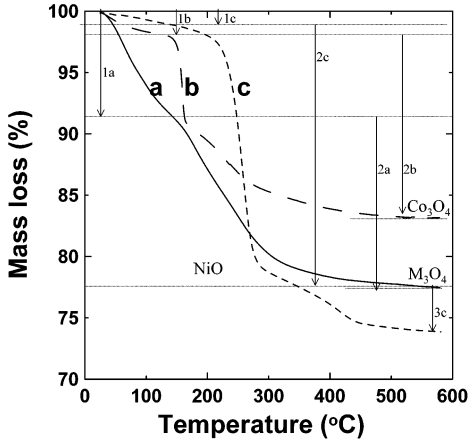

Figure 6. TGA measurements (5 K·min^{-1} in air) for $Ni_{3/8}Co_{1/4}Mn_{3/8}(OH)_2$ (a), homemade $Co(OH)_2$ (b), and commercial $Ni(OH)_2$ (c). Different mass losses indicated by arrows are explained in the text.

reveals an important and continuous mass loss, 1a (8.6%), from RT to 150 °C that could be due to loss of intercalated water or/and desorption of water molecule adsorbed on the outer surfaces of the small crystallites. Moreover, the phase with the broad peaks exists until 150 °C (Figure 5) when a spinel-type phase already begins to appear progressively.

The intermediate phase between the CdI_2-type phase and the spinel-type phase could be similar to the imperfect crystalline organization of α-nickel hydroxide.[18,20] As in this case, we expect a turbostratic structure consisting of parallel and equidistant $M(OH)_2$ ($M = Ni_xCo_{1-2x}Mn_x$) layers randomly oriented and perhaps separated by some intercalated water molecules bonded to hydroxyl groups by hydrogen bond.[18] Other authors[21] have studied a mixed Ni/Mn sample without cobalt

(19) Wyckoff, R. W. G. *Crystal Structures, Vol. 1*, 2nd ed.; Interscience Publishers: New York, 1963; p 268.

(20) McEwen, R. S. *J. Phys. Chem.* **1971**, *75*, 1782.

(21) Xu, Y.; Feng, Q.; Kajiyoshi, K.; Yanagisawa, K.; Yang, X.; Makita, Y.; Kasaishi, S.; Ooi, K. *Chem. Mater.* **2002**, *14*, 3844.

(with Ni/Mn close to 1) and describe it as a phase with stacked $Ni(OH)_2$ and MnO_2 layers. According to their X-ray diffraction diagram, however, they obtained a turbostratic phase similar to ours.

According to the literature, pure crystalline nickel hydroxide cannot be obtained by simple coprecipitation of nickel salts.[22] However, some authors have obtained a well-crystallized mixed (Co, Ni) hydroxide.[23] We have been able to obtain well-crystallized CdI_2-type mixed ($Ni_xCo_{1-2x}Mn_x$) hydroxides at RT for $0 \leq x \leq 1/2$. However, these phases show a fraction of the turbostratic phase when $x \geq 0.3$, and the fraction increases with x. To us, it seems that the well-crystallized mixed hydroxide phase is less stable at RT when the Ni (Mn) content increases and the Co content decreases.

The spinel phase appears as the drying temperature increases and remains until 600 °C and even higher. These compounds are more similar to $Co(OH)_2$ which transforms to CoO at around 900−950 °C[24] than to $Ni(OH)_2$ which transforms to NiO around 230 °C.[24] An X-ray diagram for Co_3O_4 has been placed at the top of Figure 5 for comparison. On the basis of the X-ray pattern at 600 °C, we believe that we have obtained a mixed metal spinel. Furthermore, the mass loss, 2a (13.9%) in Figure 6, also corresponds to the formation of an M_3O_4 ($M = Ni_{3/8}Co_{1/4}Mn_{3/8}$) compound.

We now compare the TGA profile of the mixed metal hydroxide to those of $Co(OH)_2$ (Figure 6b) and $Ni(OH)_2$ (Figure 6c). For $Co(OH)_2$, the weight loss 1b is 2.0%, which corresponds to adsorbed water loss. This is much smaller than the following weight loss to make Co_3O_4, 2b (14.9%). For $Ni(OH)_2$, 1c (1.2%) corresponds to the adsorbed water loss, 2c (21.2%) corresponds to the formation of NiO, and 3c (3.5%) corresponds to the beginning of calcination of NiO.[25] For $Ni_xCo_{(1-2x)}Mn_x(OH)_2$ with $x = 3/8$, the TGA profile is much more complex to interpret primarily because of the large weight loss in process 1a. Further work is needed to understand this profile fully.

Since we observed the mixed spinel $(Ni_{3/8}Co_{1/4}Mn_{3/8})_3O_4$, we heated all the mixed hydroxides, $Ni_xCo_{(1-2x)}Mn_x(OH)_2$, for the composition range $0 \leq x \leq 1/2$, overnight at 500 °C. Figure 7 shows the X-ray diffraction patterns of the heated materials. The diffraction patterns suggest that the spinel series $(Ni_xCo_{1-2x}Mn_x)_3O_4$ was obtained except for $x = 1/2$. The peaks in the diffraction patterns shift sequentially to the left as x increases. For the sample with $x = 1/2$, the pattern shows two phases: small broad peaks corresponding to a spinel-type of unknown composition and main peaks corresponding to the $NiMnO_3$ structure (space group R-3, 148). The $NiMnO_3$ phase probably has a stoichiometry that is slightly different from Ni/Mn = 1/1 to allow for the presence of the residual spinel phase that is observed.

For $0 \leq x \leq 3/8$, peaks can be indexed on the basis of the cubic spinel structure, and Figure 8 shows the lattice constant, a_0, as a function of the Ni (Mn) content, x. A linear variation typically observed for a solid solution is obtained. Because the spinel phase is not stable for the material with $x = 0.5$, it seems that the spinel structure needs the presence of a small amount of cobalt to exist.

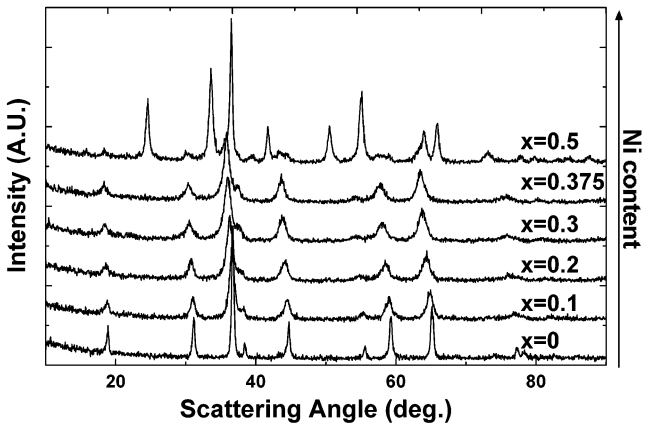

Figure 7. Powder X-ray diffraction profiles of the $Ni_xCo_{1-2x}Mn_x(OH)_2$ ($0 \leq x \leq 1/2$) samples heated to 500 °C overnight.

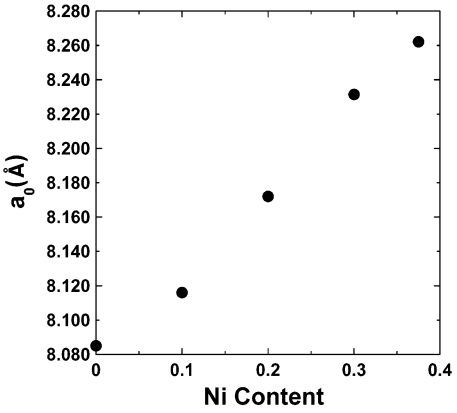

Figure 8. Lattice constant, a_0, variation obtained from the powder X-ray pattern of the $Ni_xCo_{(1-2x)}Mn_x(OH)_2$ compounds dried at 500 °C overnight ($0 \leq x \leq 3/8$), refined in the cubic cell of Co_3O_4.

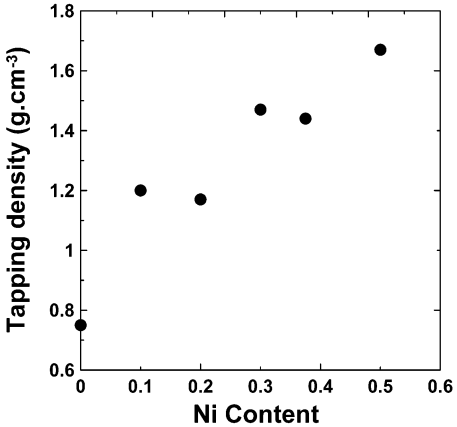

Figure 9. Tap density of $Ni_xCo_{1-2x}Mn_x(OH)_2$ ($0 \leq x \leq 1/2$) dried at 500 °C overnight.

Figure 9 shows the tap density of the $Ni_xCo_{1-2x}Mn_x(OH)_2$ ($0 \leq x \leq 1/2$) samples heated to 500 °C, plotted versus Ni (Mn) content, x. There is an increase in the tap density as a function of Ni content from 0.75 g·cm^{-3} ($x = 0$) to 1.67 g·cm^{-3} ($x = 0.5$). The tap densities are uniformly higher than those of $Ni_xCo_{1-2x}Mn_x(OH)_2$

(22) Olivia, P.; Leonardi, J.; Laurent, J. P.; Delmas, C.; Braconnier, J. J.; Filglarz, M.; Fievet, F.; de Guibert, A. *J. Power Sources* **1982**, *8*, 229.

(23) Cressent, A.; Pralong, V.; Audemer, A.; Leriche, J. B.; Delahaye-Vidal, A.; Tarascon, J. M. *Solid State Sci.* **2001**, *3*, 65.

(24) *Handbook of Chemistry and Physics*, 70th ed.; CRC Press: Boca Raton, FL, 1989−90.

(25) Freitas, M. B. J. G. *J. Power Sources* **2001**, *93*, 163.

($0 \le x \le {}^1/_2$) dried at RT (Figure 9) if we exclude the first point ($x = 0$) where the values are similar.

Conclusions

$[Ni_xCo_{1-2x}Mn_x](OH)_2$ ($0 \le x \le {}^1/_2$) phases with the CdI_2 structure were synthesized by coprecipitation, and well-crystallized compounds were obtained by drying the precipitate at room temperature. There is a linear increase in the lattice constants and tap density as x increases. These phases pass through a turbostratic phase (which is already detected in the hydroxide $Ni_xCo_{1-2x}Mn_x(OH)_2$ X-ray diffraction profile for $x \ge {}^3/_8$, too) before they transform into a spinel phase (except for $x = {}^1/_2$) upon heating.

The solid solution $(Ni_xCo_{1-2x}Mn_x)_3O_4$ ($0 \le x \le {}^3/_8$) has been prepared as well. These compounds crystallize in the spinel-type structure. Their tap densities are a little higher than those of the hydroxides dried at room temperature, and they increase as a function of Ni content. These materials could have an application in electrocatalysis, like Co_3O_4 or $NiCo_2O_4$ (which are known to be active electrocatalysts for oxygen evolution) as well as reduction in alkaline electrolyte[26] or in lithium cells.[27]

These results show the importance of the drying procedure on the $Ni_xCo_{(1-2x)}Mn_x(OH)_2$ coprecipitate. Changes to the drying temperature induce the formation of different phases. Changes to the drying procedure could have a strong impact, as a part of the first step to synthesize $Li[Ni_xCo_{(1-2x)}Mn_x]O_2$ ($0 \le x \le {}^1/_2$), on the properties (structure, composition, density, and cell performance) of the resulting oxides.

Acknowledgment. We acknowledge the support of NSERC, 3M Co., and 3M Canada Co. for the funding of this work.

CM020818E

(26) Roginskaya, Y. E.; Moroza, O. V.; Lubnin, E. N.; Ulitina, Y. E.; Lopukhova, G. V.; Trasatti, S. *Langmuir* **1997**, *13*, 4621.
(27) Larcher, D.; Sudant, G.; Leriche, J. B.; Chabre, Y.; Tarascon, J. M. *J. Electrochem. Soc.* **2002**, *149* (3), A234.